

## On the Relationship between Parametric and Geometric Active Contours

Chenyang Xu  
Center for Imaging Science  
Johns Hopkins University  
Baltimore, MD 21218

Anthony Yezzi, Jr.  
School of Elec. and Comp. Engr.  
Georgia Institute of Technology  
Atlanta, GA 30332

Jerry L. Prince  
Center for Imaging Science  
Johns Hopkins University  
Baltimore, MD 21218

**Abstract** — Geometric active contours have many advantages over parametric active contours, such as computational simplicity and the ability to change curve topology during deformation. While many of the capabilities of the older parametric active contours have been reproduced in geometric active contours, the relationship between the two has not always been clear. In this paper we develop a precise relationship between the two which includes spatially-varying coefficients, both tension and rigidity, and non-conservative external forces. The result is a very general geometric active contour formulation for which the intuitive design principles of parametric active contours can be applied. We demonstrate several novel applications in a series of simulations.

### I. INTRODUCTION

Active contours are curves that deform within digital images to recover object shapes [1]. They are classified as either *parametric active contours* (cf. [1–3]) or *geometric active contours* (cf. [4–7]) according to their representation and implementation. In particular, parametric active contours are represented explicitly as parameterized curves [1, 8] in a Lagrangian formulation. Geometric active contours are represented implicitly as level sets of two-dimensional distance functions [9–11] which evolve according to an Eulerian formulation. They are based on the theory of curve evolution implemented via level set techniques [12].

Parametric active contours are the older of the two formulations and have been used extensively in many applications over the last decade (see [13], for example). A rich variety of modifications based on physical and non-physical concepts have been implemented to solve different shape estimation problems [3, 14–16]. Geometric active contours were introduced more recently and were hailed as the solution to the problem of required topological changes during curve evolution [4, 5]. Modifications and enhancements have been added to change their behavior or improve their performance in a variety of applications [6, 7, 17–19], including a number of more global region based models which have appeared recently in the literature [35–40].

While similarities between the two active contour formulations have always been apparent, only recently have the precise relationships begun to emerge in the literature.

Caselles *et al.* [17] showed that their geometric active contours are equivalent to a special class of classical parametric active contours. Aubert and Blanc-Féraud [20] revisited this equivalence and extended it to the 3-D (active surface) case. The equivalence derived in these two cases is limited in two respects, however. First, it applies only to those active contours derived from energy minimization principles. Therefore, the question of whether a geometric formulation can be found for more general active contours is not addressed. Second, the equivalence only applies to active contours with elastic forces; rigid forces are neglected. Whitaker *et al.* [21] included rigid forces in their formulation, but only with constant weights and conservative forces.

Overall, the equivalences currently established in the literature do not relate a full family of parametric models to their geometric equivalent. As a result, it is difficult to design geometric active contours that take advantage of the wealth of parametric models that have been previously established. For example, it is not clear how one would incorporate non-conservative external forces, such as the forces defined in [16]. Also, it is not clear how to incorporate regional pressure forces, such as those used in [22, 23]. It has been well known that the use of elastic internal forces may cause undesirable shrinking effect, whereas the use of rigid internal forces can smooth the contour without this adverse effect. However, the use of rigid internal forces have been largely lacking in geometric active contour formulations so far. Since these are commonly used features in parametric active contours, there is a clear need to establish an equivalent model in geometric active contours so that the computational and topological advantages of geometric active contours can be simultaneously exploited.

In this paper, we derive an explicit mathematical relationship between the general formulations of parametric and geometric active contours. The formulation considered here allows both conservative and non-conservative external force as well as both elastic and rigid internal forces with spatially-varying weights. This equivalence relationship allows straightforward translation from almost any parametric active contour to a geometric active contour and vice versa. It does not directly apply, however, to forces that are intrinsically Lagrangian, such as the usual external spring forces or variable tension and rigidity defined on a curve parameterization. We show examples demonstrating how the more general formulation of geometric active contours

---

Please address correspondence to [prince@jhu.edu](mailto:prince@jhu.edu).

can be used to good advantage by exploiting tricks from the parametric active contour literature.

## II. BACKGROUND

### A. Parametric active contours

The classical parametric active contours, proposed by Kass *et al.* [1], are formulated by minimizing an energy functional that takes a minimum when contours are smooth and reside on object boundaries. Solving the energy minimization problem leads to a dynamic equation that has both internal and external forces. The external forces resulting from this formulation are conservative forces in that they can be written as gradients of scalar potential functions. Active contours using non-conservative forces, however, have been shown to have improved performance over traditional energy-minimizing active contours [16, 24]. Therefore, we now formulate parametric active contours directly from Newton's law, which permits use of the most general external forces.

Mathematically, a parametric active contour is a time-varying curve  $\mathbf{X}(s, t) = [X(s, t), Y(s, t)]$  where  $s \in [0, 1]$  is arclength and  $t \in \mathbf{R}^+$  is time. The dynamics of the curve are governed by the following equation

$$\gamma \mathbf{X}_t = \mathbf{F}_{\text{int}} + \mathbf{F}_{\text{ext}}, \quad (1)$$

where  $\mathbf{X}_t$  is the partial derivative of  $\mathbf{X}$  with respect to  $t$ ,  $-\gamma \mathbf{X}_t$  is the damping force with  $\gamma$  being an arbitrary non-negative constant, and  $\mathbf{F}_{\text{int}}$  and  $\mathbf{F}_{\text{ext}}$  are internal forces and external forces, respectively. The contour comes to a rest when the net effect of the damping, internal, and external forces reaches zero. The external force is designed to pull an active contour towards object boundaries or other features of interest. Many types of external forces have been developed in the past (see [41] for a comprehensive list of external forces), including the well-known pressure force [3] and the Gaussian potential force [1]. The internal force is the sum of elastic and rigid forces defined as follows

$$\mathbf{F}_{\text{elastic}} = [\alpha(s, t) \mathbf{X}_s(s, t)]_s \quad (2)$$

$$\mathbf{F}_{\text{rigid}} = -[\beta(s, t) \mathbf{X}_{ss}(s, t)]_{ss}, \quad (3)$$

where the coefficients  $\alpha(s, t)$  and  $\beta(s, t)$  can be used to control the strength of the contour's elasticity and rigidity, respectively. In this general formulation, these coefficients are allowed to vary both along the length of the curve and over time. In practice, however,  $\alpha$  is usually a positive constant and  $\beta$  is usually zero. It is important to maintain the most general formulation, however, in order to understand the precise relationship between parametric and geometric active contours.

### B. Geometric active contours

Geometric active contours [4, 5] are based on the theory of curve evolution [9–11] and the level set method [12]. In this framework, curves evolve using only geometric measures, resulting in a contour evolution that is independent of the curve's parameterization. This avoids the need to repeatedly reparameterize the curve or to explicitly handle topological changes (cf. [15, 25]). The parametric representations of the curves themselves are computed only after the evolution of the level set function is complete.

Let  $\phi(\mathbf{x}, t)$  be a 2-D scalar function whose zero level set defines the geometric active contour. The original geometric active contour formulation evolves  $\phi$  according to [4, 5]

$$\phi_t = c(\kappa + V_0)|\nabla\phi|, \quad (4)$$

where  $\kappa$  is the curvature,  $V_0$  is a constant, and

$$c \equiv c(\mathbf{x}) = \frac{1}{1 + |\nabla(G_\sigma(\mathbf{x}) * I(\mathbf{x}))|} \quad (5)$$

is an edge potential derived from the image. In (4), the product  $c(\kappa + V_0)$  determines the overall evolution speed of level sets of  $\phi(\mathbf{x}, t)$  along their normal direction. The use of curvature  $\kappa$  has the effect of smoothing the contour, while the use of  $V_0$  has the effect of shrinking or expanding contour at a constant speed. The speed of contour evolution is coupled with the image data through a multiplicative stopping term  $c$ .

This scheme works well for objects that have good contrast. When the object boundary is indistinct or has gaps, however, this contour tends to leak through the boundary. To solve this problem, the following formulation was proposed [6, 7, 17, 18]

$$\phi_t = c(\kappa + V_0)|\nabla\phi| + \nabla c \cdot \nabla\phi. \quad (6)$$

The extra stopping term  $\nabla c \cdot \nabla\phi$  is used to pull back the contour if it passes the boundary. The following model was subsequently proposed to further improve the boundary leaking problem [19]

$$\phi_t = (c\kappa|\nabla\phi| + \nabla c \cdot \nabla\phi) + V_0(c + \frac{1}{2}\mathbf{x} \cdot \nabla c)|\nabla\phi|. \quad (7)$$

The additional term  $V_0 \frac{1}{2} \mathbf{x} \cdot \nabla c |\nabla\phi|$  provides extra stopping power at boundaries.

It has been observed that even (7) does not provide a satisfactory solution to the boundary leaking problem; active contours can still leak through boundary gaps and weak edges. Several good solutions to this problem have appeared in recent parametric active contour literature [16, 22, 23]. But it is not clear, however, how these solutions can be adapted to the geometric active contour framework. In this paper, we make this connection explicit by deriving a mathematical relationship between parametric and geometric active contours. We then show how two new geometric

active contours can be obtained through this relationship, and we demonstrate how the boundary leaking problem is solved using these new active contour models. These new models complement the recent region based level set models [35–40] which also enjoy robustness against the leaking problem but which are based upon a different class of energy functionals compared to the parametric region based models we wish to extend.

### III. RELATIONSHIP BETWEEN PARAMETRIC AND GEOMETRIC ACTIVE CONTOURS

In this section, we seek to derive a general formulation for geometric active contours by reformulating (1) using a level set representation. We start by modifying the parametric problem according to the following two considerations. First, we separate pressure forces  $\mathbf{F}_{\text{pres}}(\mathbf{X})$  from other external forces  $\mathbf{F}_{\text{ext}}(\mathbf{X})$  because they require a special numerical schemes [12]. Second, we consider only the normal component of force since the tangential component affects an active contour's parameterization but not its geometry. Therefore, the class of parametric models we consider is given by

$$\gamma \mathbf{X}_t = [(\mathbf{F}_{\text{int}} + \mathbf{F}_{\text{pres}} + \mathbf{F}_{\text{ext}}) \cdot \mathbf{N}] \mathbf{N}, \quad (8)$$

where  $\mathbf{N}$  is the inward unit normal. The pressure force is given by  $\mathbf{F}_{\text{pres}} = w_{\text{pres}}(s, t) \mathbf{N}$ , which generalizes Cohen's pressure [3] by allowing the weight to be spatially and temporally varying.

#### A. Preliminaries

Next, we introduce two propositions that will be used for deriving level set formulation of internal forces.

**Proposition 1** *Let  $\mathbf{X}(s)$  be an arc-length parameterized plane curve, and let  $\mathbf{T}(s)$  and  $\mathbf{N}(s)$  be the unit tangent and unit normal vectors, respectively, such that  $\{\mathbf{T}(s), \mathbf{N}(s)\}$  form a right-handed orthonormal basis of  $\mathbf{R}^2$  for each  $s$ . Then*

- (a)  $\mathbf{X}_s(s) = \mathbf{T}(s)$ ,
- (b)  $\mathbf{T}_s(s) = \kappa(s) \mathbf{N}(s)$ , and
- (c)  $\mathbf{N}_s(s) = -\kappa(s) \mathbf{T}(s)$ .

*Proof:* (a) follows from the definition of the tangent vector and the fact that  $\mathbf{X}$  is parameterized by arclength. (b) and (c) follow from the Frenet-Serret Theorem (cf. [26]) and the fact that  $\mathbf{X}$  is a plane curve.

**Proposition 2** *Let  $\mathbf{X}(s)$  be an arc-length parameterized plane curve that coincides with a level set of the level set*

*function  $\phi(\mathbf{x}) | \mathbf{R}^2 \rightarrow \mathbf{R}$  and let  $f(\mathbf{x}) | \mathbf{R}^2 \rightarrow \mathbf{R}$  be a differentiable scalar function on the plane. Then*

$$\frac{\partial f(\mathbf{X}(s))}{\partial s} = \left[ \nabla f(\mathbf{x}) \cdot \frac{1}{|\nabla \phi(\mathbf{x})|} (-\phi_y(\mathbf{x}), \phi_x(\mathbf{x})) \right]_{\mathbf{x}=\mathbf{X}(s)}$$

*Proof:* Since  $\mathbf{X}(s)$  is a level set of  $\phi(\mathbf{x})$ ,  $\phi(\mathbf{X}(s))$  is a constant. Using the chain rule, we have

$$\phi_x X_s + \phi_y Y_s = 0. \quad (9)$$

Using the facts that  $|\mathbf{T}| = 1$ ,  $\mathbf{N} = -\nabla \phi / |\nabla \phi|$ , and  $\{\mathbf{T}(s), \mathbf{N}(s)\}$  forms a right handed orthonormal basis, we have

$$\mathbf{T} = \frac{1}{|\nabla \phi|} (-\phi_y, \phi_x). \quad (10)$$

Hence, from the chain rule

$$\frac{\partial f}{\partial s} = \nabla f \cdot \mathbf{T} = \nabla f \cdot \frac{1}{|\nabla \phi|} (-\phi_y, \phi_x)$$

which proves the proposition.

**A word about notation.** For convenience, we omitted the arguments of all functions in our proof of Proposition 2, and we will continue this practice in the sequel except where ambiguity may arise. It is a fundamental distinction that parametric active contours are Lagrangian in nature and are defined as functions of  $s$ , while geometric active contours are Eulerian in nature and are defined as functions of  $\mathbf{x}$ . To see the connection between the two, we must both *extend* functions defined on the curve to functions defined on the plane and *restrict* functions defined on the plane to functions defined on the curve (see [27] for additional details). The substitution  $\mathbf{x} = \mathbf{X}(s)$  is implied when functions defined on the plane are equated to functions defined on the curve.

#### B. Equivalence

We first focus on the internal forces in (8), which comprise both elastic and rigid forces. For the elastic forces, we use Proposition 1 to yield

$$\begin{aligned} \mathbf{F}_{\text{elastic}}(s) \cdot \mathbf{N}(s) &= [\alpha(s) \mathbf{X}_s(s)]_s \cdot \mathbf{N}(s) \\ &= [\alpha(s) \mathbf{T}(s)]_s \cdot \mathbf{N}(s) = \alpha(s) \kappa(s). \end{aligned} \quad (11)$$

Extending this result to an Eulerian representation on the plane gives

$$\mathbf{F}_{\text{elastic}}(\mathbf{x}) = \alpha(\mathbf{x}) \kappa(\mathbf{x}), \quad (12)$$

where  $\kappa(\mathbf{x})$  is given by [12]

$$\kappa = \nabla \cdot \frac{\nabla \phi}{|\nabla \phi|} = \frac{\phi_{xx} \phi_y^2 - 2\phi_x \phi_y \phi_{xy} + \phi_{yy} \phi_x^2}{(\phi_x^2 + \phi_y^2)^{3/2}}. \quad (13)$$

For the rigid forces we have

$$\begin{aligned} \mathbf{F}_{\text{rigid}}(s) \cdot \mathbf{N}(s) &= -[\beta(s)\mathbf{X}_{ss}(s)]_{ss} \cdot \mathbf{N}(s) \\ &= \beta(s)\kappa^3(s) - \rho(s), \end{aligned} \quad (14)$$

where

$$\rho(s) \stackrel{\text{def}}{=} [\beta(s)\kappa(s)]_{ss}. \quad (15)$$

Upon extending both  $\kappa$  and  $\beta$  to the plane, we use Proposition 2 to find the extension of  $\rho$  to the plane, as follows

$$\begin{aligned} \rho(\mathbf{x}) &= \nabla \left\{ \nabla \left[ \beta(\mathbf{x}) \left( \nabla \cdot \frac{\nabla \phi}{|\nabla \phi|} \right) \right] \cdot \frac{1}{|\nabla \phi|} (-\phi_y, \phi_x) \right\} \\ &\quad \cdot \frac{1}{|\nabla \phi|} (-\phi_y, \phi_x), \end{aligned} \quad (16)$$

which can also be written as

$$\rho(\mathbf{x}) = \frac{\hat{\kappa}_{xx}\phi_y^2 + \hat{\kappa}_{yy}\phi_x^2 - 2\hat{\kappa}_{xy}\phi_x\phi_y}{\phi_x^2 + \phi_y^2} - \kappa \frac{\hat{\kappa}_x\phi_x + \hat{\kappa}_y\phi_y}{(\phi_x^2 + \phi_y^2)^{1/2}} \quad (17)$$

where  $\hat{\kappa}(\mathbf{x}) = \beta(\mathbf{x})\kappa(\mathbf{x})$ . Finally, the rigid force is computed for geometric active contours using

$$\mathbf{F}_{\text{rigid}}(\mathbf{x}) = \beta(\mathbf{x})\kappa^3(\mathbf{x}) - \rho(\mathbf{x}), \quad (18)$$

where  $\rho(\mathbf{x})$  is given by (17).

We now turn to the external forces, which can be classified as either static or dynamic. Static forces are vector fields derived from the image data which do not change as the active contour deforms. Since static force fields are defined on the spatial positions rather than the active contour itself, the level set formulation of its normal component takes the following form

$$\mathbf{F}_{\text{ext}}(\mathbf{X}(s)) \cdot \mathbf{N}(s) = -\frac{1}{|\nabla \phi(\mathbf{x})|} [\mathbf{F}_{\text{ext}}(\mathbf{x}) \cdot \nabla \phi(\mathbf{x})] \quad (19)$$

Dynamic forces are those that depend on the active contour's position and orientation. The most general forces we need to consider are the spatially-varying pressure forces, whose normal component can be written as

$$\mathbf{F}_{\text{pres}}(s) \cdot \mathbf{N}(s) = w_{\text{pres}}(\mathbf{x}). \quad (20)$$

According to the fundamental relationship that a curve evolution  $\mathbf{X}_t = F(\kappa)\mathbf{N}$  can be expressed as a level set evolution  $\phi_t = F(\kappa)|\nabla \phi|$  [12], a general formula for a geometric active contour can now be derived. Substitution of the normal components for both internal and external forces into (8) and applying the fundamental relationship yields

$$\begin{aligned} \gamma \phi_t(\mathbf{x}) &= [\alpha(\mathbf{x})\kappa(\mathbf{x}) + \beta(\mathbf{x})\kappa^3(\mathbf{x}) - \rho(\mathbf{x})] |\nabla \phi(\mathbf{x})| \\ &\quad + w_{\text{pres}}(\mathbf{x}) |\nabla \phi(\mathbf{x})| - \mathbf{F}_{\text{ext}}(\mathbf{x}) \cdot \nabla \phi(\mathbf{x}) \end{aligned} \quad (21)$$

after some simplification.

Equation (21) gives a general geometric active contour formula rigorously tied to the standard parametric active contour formulation. For example, the original geometric active contour of (4) is achieved by using

$$\begin{aligned} \alpha(\mathbf{x}) &= c(\mathbf{x}), \\ \beta(\mathbf{x}) &= 0, \quad \text{and} \\ w_{\text{pres}}(\mathbf{x}) &= c(\mathbf{x})V_0. \end{aligned}$$

The geodesic active contour formulation of (6) is achieved by using

$$\begin{aligned} \alpha(\mathbf{x}) &= c(\mathbf{x}), \\ \beta(\mathbf{x}) &= 0, \\ w_{\text{pres}} &= c(\mathbf{x})V_0, \quad \text{and} \\ F_{\text{ext}}(\mathbf{x}) &= -\nabla c(\mathbf{x}). \end{aligned}$$

Finally, the extension in (7) is achieved using

$$\begin{aligned} \alpha(\mathbf{x}) &= c(\mathbf{x}), \\ \beta(\mathbf{x}) &= 0, \\ w_{\text{pres}}(\mathbf{x}) &= V_0 [c(\mathbf{x}) + \frac{1}{2} \mathbf{x} \cdot \nabla c(\mathbf{x})], \quad \text{and} \\ F_{\text{ext}}(\mathbf{x}) &= -\nabla c(\mathbf{x}). \end{aligned}$$

It is apparent from this comparison that previous creativity in the development of new geometric active contours has been somewhat limited. For example, pressure forces have typically been tied through  $c(\mathbf{x})$ , the edge potential, to internal tension forces. External forces have been limited to irrotational forces, and these also tied to  $c(\mathbf{x})$ . Finally, the use of rigid forces has been largely missing in existing geometric active contours. There is room for much creativity in the selection of parameters for a geometric active contour, and the derived equivalence should help to identify the opportunities and their relation to parametric active contours. We explore some possibilities in the Applications section.

### C. Implementation Issues

We implemented the geometric active contour of (21) using the narrow band approach described in [28]. Rebuilding the narrow band when the contour hits the narrow band boundary is calculated using the fast marching algorithm described in [29, 30]. To assure the stability of the algorithm, the rigid force is computed based on the algorithm proposed by Chopp and Sethian [31].

### D. Remarks

The relationship we have derived does not provide a complete equivalence. From the outset we eliminated all terms that depend on an explicit parameterization of the active contour. But a parameterization is required for certain parametric active contours. For example, spring forces

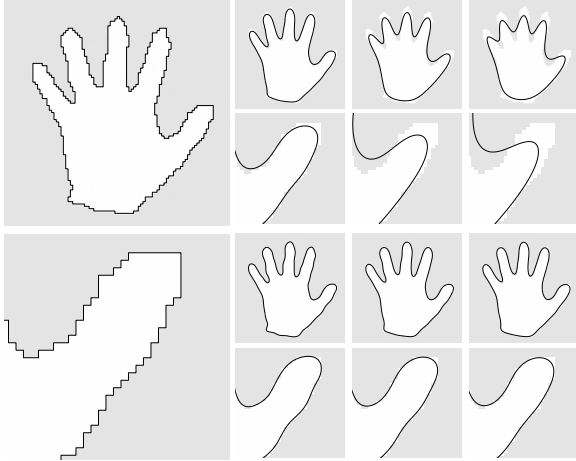


Fig. 1: A jagged hand contour (top left) and a zoom up around the thumb (bottom left). Top row right: active contour deformed under elastic force with  $\alpha = 0.1$  for 100, 500, and 1000 iterations. Bottom row right: active contour deformed under rigid force with  $\beta = 0.1$  for 100, 500, and 1000 iterations.

use springs that are tied to particular points on the contour (cf. [1]). They are Lagrangian in character, and it would require contour point tracking to implement them within an Eulerian framework. Active contours that mimic physical objects whose tension and rigidity coefficients vary along the curve likewise cannot be implemented without contour point tracking. So, to complete the equivalence, some way to keep track of the initial coordinate  $s$ , given the spatial location  $\mathbf{x}$  of an active contour is required. This is a subject for future research.

#### IV. APPLICATIONS

This section shows the application of the mathematical relationship derived in Section III for designing new geometric active contours based on two recent parametric active contours.

**Contour fairing.** It has sometimes been argued that the active contour rigidity term is not necessary, that the elasticity term is adequate [17]. But the elasticity term shrinks contours, which may be undesirable in some applications. Use of the rigidity term (non-zero  $\beta$ ) with small or no elasticity can help provide contour smoothness — fairing the contour — while minimizing contour shrinkage. Equation (21) provides a way to do this within the geometric active contour framework. Fig. 1 contrasts the contour smoothing difference between elastic forces and rigid forces.

**Region-based forces.** Region information — e.g., from image segmentation — can be used to improve the robustness of an active contour, both to noise and to weak edges.

Those parametric active contours formulations that have incorporated region information — e.g., [22,23,32,33] — can all be written in the following way

$$\gamma \mathbf{X}_t = [\alpha(s) \mathbf{X}_s]_s - [\beta(s) \mathbf{X}_{ss}]_{ss} + w_R R(\mathbf{X}) \mathbf{N} + \mathbf{F}_{\text{ext}}(\mathbf{X}), \quad (22)$$

where  $R(\mathbf{x})$  is a *region function* and  $w_R$  is a positive weighting parameter. The region function is derived from the image and (for the sake of concreteness) has values in the range  $[-1,1]$  that are smaller within the region(s)-of-interest. The region function modulates the sign of the pressure forces using region information so that the contour shrinks when it is outside the object of interest and expands when it is inside the object. For this reason, these external forces are sometimes called *signed pressure forces*.

Signed pressure forces help to solve the so-called boundary leaking problem, which results from weak edges. This idea has only recently been incorporated into geometric active contours [34–36], and our equivalence relationship permits a direct and more general result. In particular, using (8) and (21), we can easily write

$$\gamma \phi_t(\mathbf{x}) = [\alpha(\mathbf{x}) \kappa(\mathbf{x}) + \beta(\mathbf{x}) \kappa^3(\mathbf{x}) - \rho(\mathbf{x})] |\nabla \phi(\mathbf{x})| + w_R R(\mathbf{x}) |\nabla \phi(\mathbf{x})| - \mathbf{F}_{\text{ext}}(\mathbf{x}) \cdot \nabla \phi(\mathbf{x}), \quad (23)$$

which comprises a more general class of region-based, geometric active contours than has previously been reported. See [35–40] for some other, more specialized, region-based geometric active contour models.

**Gradient vector flow forces.** Active contours using gradient vector flow external forces have been shown to have a larger capture range and the ability to converge into boundary concavities [16]. They have been used only in parametric active contour formulations, however, because they comprise non-conservative forces that do not fit within the standard geometric (or geodesic) active contour framework. Using our derived equivalence, it is straightforward to develop a gradient vector flow active contour.

A GVF field is defined as the equilibrium solution of a generalized vector diffusion equation

$$\mathbf{v}_t = g(|\nabla f|) \nabla^2 \mathbf{v} - h(|\nabla f|) (\mathbf{v} - \nabla f), \quad (24)$$

where  $\mathbf{v}(\mathbf{x}, 0) = \nabla f$ ,  $\mathbf{v}_t$  denotes the partial derivative of  $\mathbf{v}(\mathbf{x}, t)$  with respect to  $t$ ,  $\nabla^2$  is the Laplacian operator (applied to each spatial component of  $\mathbf{v}$  separately), and  $f$  is an edge map that has a higher value at the desired object boundary. The functions  $g(r)$  and  $h(r)$  control the amount of diffusion in GVF; in this paper, we use  $g(r) = \exp\{-(r/\kappa)^2\}$  and  $h(r) = 1 - g(r)$ , where  $\kappa$ . We define  $\tilde{\mathbf{v}} = \mathbf{v}(\mathbf{x}, \infty)$ , the equilibrium state of (24). A general geometric GVF active contour follows by substituting

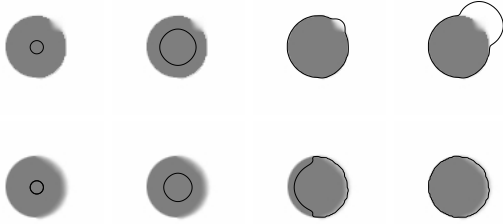


Fig. 2: Top row: standard geometric active contour. Bottom row: region-based geometric active contour using new equivalence formulation.

$\tilde{v}(\mathbf{x})$  for  $\mathbf{F}_{\text{ext}}(\mathbf{x})$  in (23), yielding

$$\begin{aligned} \gamma\phi_t(\mathbf{x}) = & [\alpha(\mathbf{x})\kappa(\mathbf{x}) + \beta(\mathbf{x})\kappa^3(\mathbf{x}) - \rho(\mathbf{x})]|\nabla\phi(\mathbf{x})| \\ & + w_R R(\mathbf{x})|\nabla\phi(\mathbf{x})| - \tilde{v}(\mathbf{x}) \cdot \nabla\phi(\mathbf{x}). \end{aligned} \quad (25)$$

If desired or necessary, region forces can be turned off by setting  $w_R = 0$ .

**Volcano forces.** Volcano forces are local repulsive forces that are determined by a volcano location specified by the user [1]. They are a powerful tool for interactive snake manipulation commonly used in parametric snakes. They are readily implemented as static external forces and either add to or replace  $\mathbf{F}_{\text{ext}}$ .

#### A. Examples

Figure 2 shows an example patterned after one in [19], in which there is a weak boundary at the top right of the circle. The top row of this figure shows a conventional geometric active contour leaking through this boundary, while the bottom row shows a region-based geometric active contour implemented using (23). To construct the region function in this example, we applied fuzzy C-means to automatically classify the figure into two classes, each with a fuzzy membership value at each pixel. The region function was then given by

$$R(\mathbf{x}) = 1 - 2\mu_d(\mathbf{x}). \quad (26)$$

where  $\mu_f(\mathbf{x})$  is the membership function corresponding to the darker intensity class. These experiments also used an additional external force given by

$$\mathbf{F}_{\text{ext}}(\mathbf{x}) = \nabla\mu_f(\mathbf{x}). \quad (27)$$

Fig. 3 shows our region-based geometric active contour converging from a single initialization to the ventricles in the top row and the gray matter/white matter interface in the second row. The only difference between the two formulations is in the region function, which was based on the ventricle fuzzy membership in the top row and the white matter fuzzy membership in the bottom row.

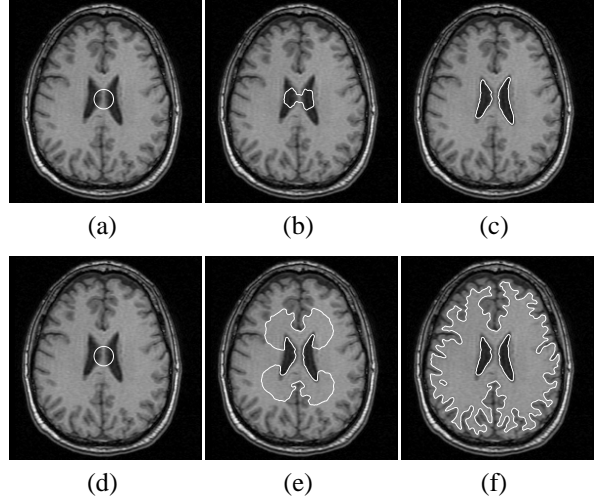


Fig. 3: A region-based geometric active contour can extract either the ventricle (top row) or the white matter (bottom row).

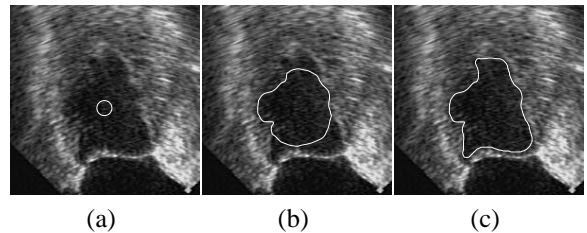


Fig. 4: Segmentation of the LV on a cardiac ultrasound image from a single geometric GVF active contour.

Gradient vector flow is very useful when there are boundary gaps, because it preserves the perceptual edge property of snakes [1, 16]. Figure 4 shows a geometric GVF snake applied to a noisy ultrasound image of the left ventricle. We note that the standard geodesic active contour of [6] or [7] failed to produce the correct result on this image.

#### V. SUMMARY AND CONCLUSION

We have derived an explicit mathematical relationship between the general formulations of parametric and geometric active contours. This relationship highlights the Lagrangian nature of parametric active contours and the Eulerian nature of geometric active contours. Of particular note is the inclusion of rigidity in this equivalence. Described applications of the relationship include curve fairing, region-based and gradient vector flow active contours, and interactive volcano forces. Examples on simulated and real images were presented, demonstrating in particular its effectiveness on the boundary leaking problem. We anticipate that new geometric active contours will be developed using the equivalence derived in this paper. Extending this relationship to 3-D should be relatively straightforward.

#### ACKNOWLEDGMENTS

The authors thank Xiao Han for his assistance in implementing the geometric active contours using the narrow-band method and Dzung Pham for providing the fuzzy c-means algorithm. The work was supported in part by an NSF/ERC grant CISST-9731748 and NIH/NINDS grant R01NS37747.

## REFERENCES

- [1] M. Kass, A. Witkin, and D. Terzopoulos. Snakes: active contour models. *Int'l J. Comp. Vis.*, 1(4):321–331, 1987.
- [2] A. A. Amini, T. E. Weymouth, and R. C. Jain. Using dynamic programming for solving variational problems in vision. *IEEE T. Patt. Anal. Mach. Intell.*, 12(9):855–867, 1990.
- [3] L. D. Cohen. On active contour models and balloons. *CVGIP: Imag. Under.*, 53(2):211–218, 1991.
- [4] V. Caselles, F. Catte, T. Coll, and F. Dibos. A geometric model for active contours. *Numerische Mathematik*, 66:1–31, 1993.
- [5] R. Malladi, J. A. Sethian, and B. C. Vemuri. Shape modeling with front propagation: a level set approach. *IEEE T. Patt. Anal. Mach. Intell.*, 17(2):158–175, 1995.
- [6] V. Caselles, R. Kimmel, and G. Sapiro. Geodesic active contours. In *Proc. Int'l Conf. Comp. Vis.*, pages 694–699, 1995.
- [7] A. Yezzi, S. Kichenassamy, A. Kumar, P. Olver, and A. Tannenbaum. A geometric snake model for segmentation of medical imagery. *IEEE T. Med. Imag.*, 16:199–209, 1997.
- [8] D. Terzopoulos and K. Fleischer. Deformable models. *The Visual Computer*, 4:306–331, 1988.
- [9] G. Sapiro and A. Tannenbaum. Affine invariant scale-space. *Int'l J. Comp. Vis.*, 11(1):25–44, 1993.
- [10] L. Alvarez, F. Guichard, P. L. Lions, and J. M. Morel. Axioms and fundamental equations of image processing. *Arch. Rational Mech. Anal.*, 123(3):199–257, 1993.
- [11] B. B. Kimia, A. R. Tannenbaum, and S. W. Zucker. Shapes, shocks, and deformations I: the components of two-dimensional shape and the reaction-diffusion space. *Int'l J. Comp. Vis.*, 15:189–224, 1995.
- [12] S. Osher and J. A. Sethian. Fronts propagating with curvature-dependent speed: algorithms based on Hamilton-Jacobi formulations. *J. Comp. Physics*, 79:12–49, 1988.
- [13] T. McInerney and D. Terzopoulos. Deformable models in medical image analysis: a survey. *Med. Imag. Anal.*, 1(2):91–108, 1996.
- [14] L. H. Staib and J. S. Duncan. Boundary finding with parametrically deformable models. *IEEE T. Patt. Anal. Mach. Intell.*, 14(11):1061–1075, 1992.
- [15] R. Durikovic, K. Kaneda, and H. Yamashita. Dynamic contour: a texture approach and contour operations. *The Visual Computer*, 11:277–289, 1995.
- [16] C. Xu and J. L. Prince. Snakes, shapes, and gradient vector flow. *IEEE T. Imag. Proc.*, 7(3):359–369, 1998.
- [17] V. Caselles, R. Kimmel, and G. Sapiro. Geodesic active contours. *Int'l J. Comp. Vis.*, 22:61–79, 1997.
- [18] S. Kichenassamy, A. Kumar, P. Olver, A. Tannenbaum, and A. Yezzi. Conformal curvature flows: from phase transitions to active vision. *Arch. Rational Mech. Anal.*, 134:275–301, 1996.
- [19] K. Siddiqi, Y. B. Lauzière, A. Tannenbaum, and S. W. Zucker. Area and length minimizing flows for shape segmentation. *IEEE T. Imag. Proc.*, 7:433–443, 1998.
- [20] G. Aubert and L. Blanc-Féraud. Some remarks on the equivalence between 2D and 3D classical snakes and geodesic active contours. *Int'l J. Comp. Vis.*, 34:19–28, 1999.
- [21] R.T. Whitaker and D.T. Chen. Embedded active surfaces for volume visualization. Technical Report ECRC-94-8, European Computer-Industry Research Centre GmbH, 1994.
- [22] R. Ronfard. Region-based strategies for active contour models. *Int'l J. Comp. Vis.*, 13(2):229–251, 1994.
- [23] C. S. Poon and M. Braun. Image segmentation by a deformable contour model incorporating region analysis. *Phys. Med. Biol.*, 42:1833–1841, 1997.
- [24] C. Xu and J. L. Prince. Generalized gradient vector flow external forces for active contours. *Signal Processing — An International Journal*, 71(2):131–139, 1998.
- [25] T. McInerney and D. Terzopoulos. Topologically adaptable snakes. In *Proc. Int'l Conf. Comp. Vis.*, pages 840–845, 1995.
- [26] R. S. Millman and G. D. Parker. *Elements of Differential Geometry*. Prentice-Hall, Englewood Cliffs, NJ, 1977.
- [27] J. A. Sethian. *Level Set Methods and Fast Marching Methods: Evolving Interfaces in Computational Geometry, Fluid Mechanics, Computer Vision, and Material Science*. Cambridge University Press, Cambridge, UK, 2nd edition, 1999.
- [28] D. Adalsteinsson and J. A. Sethian. A fast level set method for propagating interfaces. *J. Comp. Phys.*, 118(2):269–277, 1995.
- [29] J. A. Sethian. A fast marching level set method for monotonically advancing fronts. *Proc. Nat. Acad. Sci.*, 93(4):1591–1595, 1996.
- [30] D. Adalsteinsson and J. A. Sethian. The fast construction of extension velocities in level set methods. *J. Comp. Phys.*, 148(1):2–22, 1999.
- [31] D. L. Chopp and J. A. Sethian. Motion by intrinsic laplacian of curvature. *Interfaces and Free Boundaries*, 1(1):107–123, June 1999.
- [32] S. Zhu and A. Yuille. Region competition: Unifying snakes, region growing, and byes/mdl for multiband image segmentation. *IEEE T. Patt. Anal. Mach. Intell.*, 18(9):884–900, 1996.
- [33] A. Chakraborty, L. H. Staib, and J. S. Duncan. Deformable boundary finding in medical images by integrating gradient and region information. *IEEE T. Med. Imag.*, 15(6):859–870, 1996.
- [34] N. Paragois and R. Deriche. Detecting multiple moving targets using deformable contours. In *Proc. Int'l Conf. Imag. Proc.*, pages 183–186, 1997.
- [35] N. Paragois and R. Deriche. Unifying boundary and region-based information for geodesic active tracking. In *Proc. Comp. Vis. Patt. Recog.*, pages 300–305, 1999.
- [36] N. Paragios and R. Deriche. Geodesic active contours and level sets for the detection and tracking of moving objects. *IEEE T. Patt. Anal. Mach. Intell.*, 22(3):1–15, 2000.
- [37] T. Chan and L. Vese, “Active contours without edges,” To appear in *IEEE Trans. Image Processing*.
- [38] C. Samson, L. Blanc-Feraud, G. Aubert, and J. Zerubia. “A Level Set Method for Image Classification,” *Int. Conf. Scale-Space Theories in Computer Vision*, pp. 306–317, 1999.
- [39] A. Yezzi, A. Tsai, and A. Willsky, “A Statistical Approach to Image Segmentation for Bimodal and Trimodal Imagery,” *Proceedings of ICCV*, September, 1999.
- [40] A. Yezzi, A. Tsai, and A. Willsky, “A Fully Global Approach to Image Segmentation via Coupled Curve Evolution Equations,” To appear in *J. of Visual Communication and Image Representation*.
- [41] C. Xu, D. L. Pham, and J. L. Prince, “Image Segmentation Using Deformable Models,” *Handbook of Medical Imaging: Vol. 2. Medical Image Processing and Analysis*, SPIE Press, 2000.